Estimation of skin concentrations of topically applied lidocaine at each depth profile

Takeshi Oshizaka[a], Keisuke Kikuchi[a], Wesam R. Kadhum[a], Hiroaki Todo[a], Tomomi Hatanaka[a,b], Konstanty Wierzba[a], Kenji Sugibayashi[a,*]

[a]*Faculty of Pharmaceutical Sciences, Josai University, 1-1 Keyakidai, Sakado, Saitama 350-0295, Japan*

[b]*Tokai University Institute of Innovative Science and Technology, 4-1-1 Kitakaname, Hiratsuka, Kanagawa 259-1292, Japan*

[*]Corresponding author: Faculty of Pharmaceutical Sciences, Josai University, 1-1 Keyakidai, Sakado, Saitama 350-0295, Japan. Tel.: +81 49 271 7367; fax: +81 49 271 8137.

E-mail address: sugib@josai.ac.jp (K. Sugibayashi).

ABSTRACT

Skin concentrations of topically administered compounds need to be considered in order to evaluate their efficacies and toxicities. This study investigated the relationship between the skin permeation and concentrations of compounds, and also predicted the skin concentrations of these compounds using their permeation parameters. Full-thickness skin or stripped skin from pig ears was set on a vertical-type diffusion cell, and lidocaine (LID) solution was applied to the stratum corneum (SC) in order to determine *in vitro* skin permeability. Permeation parameters were obtained based on Fick's second law of diffusion. LID concentrations at each depth of the SC were measured using tape-stripping. Concentration-depth profiles were obtained from viable epidermis and dermis (VED) by analyzing horizontal sections. The corresponding skin concentration at each depth was calculated based on Fick's law using permeation parameters and then compared with the observed value. The steady state LID concentrations decreased linearly as the site became deeper in SC or VED. The calculated concentration-depth profiles of the SC and VED were almost identical to the observed profiles. The compound concentration at each depth could be easily predicted in the skin using diffusion equations and skin permeation data. Thus, this

method was considered to be useful for promoting the efficient preparation of topically applied drugs and cosmetics.

Keywords:

Concentration-distance profile

Permeation parameter

Skin concentration

Skin permeation

Lidocaine

Chemical compounds examined in this study

Lidocaine (PubChem CID: 3676); Lidocaine hydrochloride monohydrate (PubChem CID: 16219577)

1. Introduction

The efficacy and toxicity of active compounds have been classified into direct and indirect reactions. A direct reaction is caused by a compound directly binding to the receptor, and the relationship between the reaction and concentration of the compound can be described by Hill's equation (Kano et al., 2006). Although indirect reactions have been attributed to the promotion or inhibition of enzymatic reactions by an active compound, the reaction itself is also a function of the concentration of the compound. Thus, accurately measuring the concentrations of active molecules at the site of action enables a high precision prediction for their efficacies and toxicities.

Two main sites of action have been identified for compounds that are absorbed into the body through the skin. One is sites apart from the skin while the other is the skin itself. In the former case, a compound is absorbed through the skin and then carried to the site of action by the blood circulation. The concentrations of active molecules at the site of action have generally been described as a function of the blood concentration (Huffman et al., 1976; Sheiner et al., 1977; Vozeh et al., 1985). Moreover, blood concentration-time curves can be predicted using skin permeation parameters, such as the flux and permeability coefficient, which are obtained from *in*

vitro skin permeation experiments (Sato et al., 1988a; Sato et al., 1988b; Hatanaka et al., 1994; Nakamura et al., 2012). Skin permeation behaviors and blood concentration profiles for compounds having sites of action other than the skin need to be elucidated in more detail.

On the other hand, the importance of the skin concentration is greater than that of skin permeation behavior for topical drugs, cosmetics, and compounds that are capable of causing skin irritation and inflammation. A large number of sites of action have been identified, from the skin surface for sunscreens and skin protective agents to the viable epidermis and dermis (VED) for antimicrobials, antipruritics, and functional cosmetics. Therefore, the concentration at each skin depth is needed in order to evaluate the efficacy and safety of topically active compounds.

The skin concentrations of compounds have been measured using various methods; suction blister (Kiistala, 1968), punch and shave biopsies (Surber et al., 1993), heating (Surber et al., 1990), autoradiography (Schaefer et al., 1978), tape-stripping (Pershing et al., 1992; Rougier et al., 1983; Tojo and Lee, 1989; N'Dri-Stempfer et al., 2009) and Raman spectrophotometry (Lademann et al., 2012). However, these evaluation methods are problematic for various reasons such as the difficulties associated with using human skin, incomplete removal of the applied formulation from

the skin surface, and low extraction ratio of compounds from the skin. Furthermore, measuring skin concentrations at each depth is more difficult than determining mean concentrations in the whole skin.

We previously demonstrated that the mean concentration in the whole skin during steady state permeation could be predicted from skin permeation parameters based on Fick's second law of diffusion (Sugibayashi et al., 2010). In the present study, we attempted to establish an accurate and convenient method for predicting skin concentration-depth profiles during steady state permeation based on the skin permeation parameters of topically active compounds.

2. Materials and methods

2.1.Materials

Lidocaine (LID) hydrochloride monohydrate and mepivacaine hydrochloride were purchased from Sigma Aldrich (St. Louis, MO, U.S.A.). 4-Hydroxy benzoic acid and sodium 1-heptanesulfonate were obtained from Tokyo Chemical Industry Co., Ltd. (Tokyo, Japan). Ammonium acetate was obtained from Wako Chemical Industries,

Ltd. (Osaka, Japan). Other chemicals and reagents were of special grade or HPLC grade commercially obtained and used without further purification. The frozen ears of male and female pigs (LWD, 6-12 month) were obtained from Saitama Experimental Animals Supply Co., Ltd. (Saitama, Japan). The skin was stored at -80°C until permeation experiments.

2.2.Skin permeation experiments

Frozen pig ears were thawed at 32°C and full-thickness skin was excised after being cleaned with pH 7.4 phosphate-buffered saline (PBS). Stripped skin was obtained by tape-stripping the stratum corneum (SC) 30 times with adhesive tape prior to its excision from the pig ear (Klang et al., 2012). Excess fat was trimmed off from the excised skin, and the skin sample was set in a vertical-type diffusion cell (effective diffusion area, 1.77 cm^2) in which the receiver chamber was warmed to 32°C. After a 1-h equilibration period with PBS, pH 5.0, 7.4, or 10 PBS containing 1.0 mg/mL of LID (volume; 1.0 mL) was applied to the SC side as a donor solution, and pH 7.4 PBS (volume; 6.0 mL) was added to the VED side as a receiver solution. The receiver solution was stirred with a stirrer bar on a magnetic stirrer and maintained at 32°C throughout the experiments. An aliquot (500 μL) was withdrawn from the receiver

chamber and the same volume of PBS was added to the chamber to keep the volume constant. The penetrant concentration in the receiver chamber was determined by HPLC or LC/MS/MS.

2.3.Measurement of skin pH

The pH values of the surface (SC for full-thickness skin and viable epidermis for stripped skin or full-thickness skin after tape-stripping) and dermis sides of the skin were measured before and after skin permeation experiments by a Skin-pH meter (Derma Unit SCC3; Courage+Khazaka Co., Cologne, Germany).

2.4.Determination of skin concentrations

2.4.1. LID concentration-depth profile of SC

LID concentrations were measured at various depths of the SC during steady state permeation according to the method of N'Dri-Stempfer et al. (2009). The donor solution for the skin permeation experiment was removed and the SC side was rinsed three times with 1.0 mL of PBS. The SC was removed by the sequential application and removal of adhesive tape (Cellotape® CT-15, Nichiban, Tokyo, Japan). Each tape

was immersed in 1.0 mL of PBS for 1 h to extract LID. LID in the extraction liquids was analyzed by HPLC. The amount of the SC removed was different with each tape-stripping; therefore, the total thickness of the SC (L_{sc}) and thickness of the remaining SC (L_{sc}-x) was estimated based on the change in transepidermal water loss (TEWL), i.e. (Kalia et al., 1996),

$$TEWL = \frac{K_w D_w \Delta C}{L_{sc} - x} \quad (1)$$

where K_w is the partition coefficient of water between the SC and epidermis, D_w is the diffusion coefficient of water in the SC, ΔC is the concentration difference across the SC and x is the thickness of the SC removed by tape-stripping, which is calculated from the gain in mass of adhesive tapes assuming 1.0 g/cm^3 of SC density . The plot of reciprocal of TWEL versus x is linear and the slope and intercept yield L_{sc} value (L_{sc} = - intercept / slope).

2.4.2. LID concentration-depth profile of VED

After skin permeation reached a steady state, the donor solution was removed and both the SC and VED sides were washed with PBS. The SC was removed by tape-stripping and the remaining VED was frozen using dry ice. The frozen VED was vertically cut to an approximately 0.5 cm square using a razor blade, embedded in super

cryoembedding medium (Leica Microsystems, Tokyo, Japan), and frozen quickly in isopentane cooled with dry ice. A cryostat (CM3050S, Leica Microsystems) was used to prepare horizontal slices of the VED. Each of the 200-μm thick serial VED slices was placed into a microtube and LID was extracted by immersing the slices in 1.0 mL of PBS for 1 h. LID in the extraction liquids was analyzed by LC/MS/MS. When the LID concentration in the first and second slices, the rippled layer of viable epidermis immediately under the SC, was high more than 10 times of that in next slices, it was considered to be the insufficient SC removal and excluded from the data.

2.5.Analytical methods for LID

2.5.1. HPLC

The withdrawn sample containing LID (200 μL) was mixed with 200 μL acetonitrile containing an internal standard (4-hydroxy benzoic acid) and centrifuged at 4°C for 5 min. The obtained supernatant (20 μL) was injected into an HPLC system. The HPLC system (Shimadzu; Kyoto, Japan) consisted of a system controller (CBM-20A), pump (LC-20AD), auto-sampler (SIL-20AC), column oven (CTO-20A), UV detector (SPD-M20A), and analysis software (LC Solution). The column was

Inertsil® ODS-3 4.6 mm×150 mm (GL Sciences Inc.; Tokyo, Japan), which was maintained at 40°C. The mobile phase was 0.1% phosphoric acid in water : acetonitrile = 7 : 3 containing 5.0 mM sodium 1-heptanesulfonate, and the flow rate was adjusted to 1.0 mL/min. LID was detected at UV 230 nm.

2.5.2. LC/MS/MS

The withdrawn sample containing LID (200 μL) was mixed with 200 μL acetonitrile containing an internal standard (mepivacaine) and centrifuged at 4°C for 5 min. The obtained supernatant (10 μL) was injected into an LC/MS/MS system. The LC/MS/MS system consisted of a system controller (CBM-20A; Shimadzu), pump (LC-20AD; Shimadzu), auto-sampler (SIL-20AC$_{HT}$; Shimadzu), column oven (CTO-20A; Shimadzu), detector (4000QTRAP; AB Sciex, Tokyo, Japan), and analysis software (Analyst® version1.4.2; Shimadzu). The column was Shodex ODP2 HP-2B 2.0 mm×50 mm (Showadenko Inc.; Tokyo, Japan), which was kept at 40°C. The mobile phase was 10 mM ammonium acetate in water : acetonitrile = 7 : 3, and the flow rate was 0.2 mL/min.

2.6.Prediction of skin concentrations

Fig. 1 shows a schematic diagram of the concentration-depth profiles for two-layered diffusion models consisting of the SC and VED for skin permeation (Sugibayashi et al., 2010). The vertical and horizontal axes indicate the concentration of the penetrant and depth from the skin surface, respectively. The hatched area shows the amount of penetrant in a unit area of the skin, and the product of the diffusion coefficient and slope of the VED layer was used to determine the permeation rate. The concentration of the penetrant at position x in the SC ($0 \leq x \leq L_{sc}$) under steady state permeation ($C_{sc,ss}$) can be represented by

$$C_{sc,ss} = K_{sc}C_v - \frac{K_{sc}C_v}{L_{sc}}\left(1 - \frac{P_{tot}}{P_{ved}}\right)x \quad (2)$$

where C_v is the applied concentration of the penetrant in the vehicle, K_{sc} is the partition coefficient from vehicle to the SC, P_{tot} and P_{ved} are the permeability coefficients through full-thickness and stripped skin, respectively, and L_{sc} is the thickness of the SC.

The steady state concentration of the penetrant at position x in the VED ($C_{ved,ss}$, $L_{sc} \leq x \leq L_{sc}+L_{ved}$) is expressed as

$$C_{ved,ss} = K_{ved}C_v \frac{P_{tot}}{P_{ved}}\left(\frac{L_{sc} + L_{ved} - x}{L_{ved}}\right) \quad (3)$$

where K_{ved} is the partition coefficient of the penetrant from vehicle to the VED and L_{ved} is the thickness of the VED.

Skin permeation parameters, which were required to predict the penetrant

concentration at each depth of the VED (P_{ved} and K_{ved}), could be obtained by fitting permeation data through stripped skin to the one-layered diffusion model (Ohmori et al., 2000). The parameters for SC (P_{sc} and K_{sc}) were then calculated in the SC by fitting permeation data through full-thickness skin to the two-layered diffusion model using fixed values for P_{ved} and K_{ved}. These model adaptations were carried out by the weighted least-square method using a quasi-Newton algorithm on solver-function of Microsoft Excel 2007. The steady state concentration ($C_{sc,ss,}$ and $C_{ved,ss}$) – skin depth (x) profile was calculated from equations (2) and (3) using the fixed values of skin permeation parameters and thicknesses (L_{ved} and L_{sc}).

Fig. 1

3. Results

3.1.Skin permeation of LID

3.1.1. Effect of pH on the skin permeation of LID

Fig. 2 shows the cumulative amount of LID that permeated through

full-thickness and stripped skin from donor solutions at several pH values. The permeation of LID through both types of skin was high in the order of pH 10, pH 7.4, and pH 5.0. However, differences among pH values were lower for stripped skin than for full-thickness skin. The permeation parameters P_{tot}, P_{ved}, K_{sc}, and K_{ved} were calculated by fitting data in Fig. 2 to diffusion models (Ohmori et al., 2000) and are listed in Table 1. The parameter values for pH 7.4 were similar to those for pH 10. When these values were compared with those for pH 5.0, P_{tot} and K_{tot} were 52 and 81 times higher, respectively. The similar tendencies were observed in P_{ved} and K_{ved} values, although the differences between pH 5.0 and the other pHs were smaller than those in P_{tot} and $K_{tot.}$

Fig. 2

Table 1

3.1.2. Changes in skin pH after permeation

The pH values of the surface (SC for full-thickness skin and viable epidermis for stripped skin or full-thickness skin after tape-stripping) and dermis sides of the skin before and after permeation experiments are listed in Table 2. The pH values of the

VED in full-thickness skin before and after the permeation experiments were approximately 7.4, regardless of the applied donor solutions. The values for stripped skin were also approximately 7.4, except for the donor solution at pH 10.

Subsequent skin concentration-depth profiles under steady state permeation were predicted at pH 7.4 because of the low skin permeability observed at pH 5.0 and changes in skin pH at pH 10.

Table 2

3.2.Skin concentration of LID under steady state permeation

3.2.1. LID concentration-SC depth profile

Steady state LID concentrations were measured at various depths in the SC after skin permeation experiments, in which pH 7.4 donor solution was applied for 8 h, and plotted with the calculated values in Fig. 3. The calculation was performed using equation (2) with permeation parameters obtained from the corresponding skin permeation data in Fig. 2. Due to differences in the thickness of the SC among skins, data for individual skins are shown in Fig. 3a-c, whereas data for all skin, in which the

depth was normalized by the thickness of the SC, are shown in Fig. 3d. The steady state LID concentration in the SC decreased linearly as permeation deepened. The calculated LID concentration-depth profile was almost the same as the observed profile.

Fig. 3

Fig. 4 shows the relationship between the observed and calculated values for steady state LID concentrations at various depths in the VED following the application of pH 7.4 donor solution. Permeation parameters, which were obtained from the corresponding permeation experiments through full-thickness and stripped skins (Fig. 2), were used in the calculation using equation (3). The thickness of the VED was different among skins, which was similar to that observed in the SC; therefore, the raw data for each skin are shown in Fig. 4a-e and data normalized by depth VED thickness are shown in Fig. 4f. The concentration of LID decreased linearly as the site became deeper. The calculation performed based on permeation data provided an almost identical concentration-depth profile to the observed profile.

Fig. 4

Fig. 5 shows the steady state LID concentration-depth profile for full-thickness skin, which was constructed by combining the data in Fig. 3d with those in Fig. 4f. The concentration gradient was significantly higher in the SC than in the VED. The profile was a typical one of the two-layered skin model shown in Fig. 1.

Fig. 5

4. Discussion

The efficacies and toxicities of topically applied drugs and cosmetics are determined by their concentrations in the skin, and sites of action are distributed over a wide area of the skin. Melanin, which causes pigmentation, is produced by melanosomes in the basal layer of the viable epidermis (Seiji et al., 1961). Effective concentrations of arbutin (Maeda and Fukuda, 1996) and kojic acid (Mishima et al., 1988) are required in the viable epidermis in order to inhibit melanin production. Vitamin A has been shown to improve blood flow (Kligman, 1989) and, thus, its efficacy is affected by its concentration in the dermis. Therefore, knowing the

concentrations of active compounds in the skin, especially the target tissue, is of importance.

LID is mainly used as an antiarrhythmic or topical anesthetic, and transdermal tape has also been developed for the treatment of neuralgia and numbness in the limbs. Since its molecular weight is 234.34 and logarithm of the octanol/PBS partition coefficient is 0.23 (32°C), the skin permeability of LID is relatively high (Bos and Meinardi, 2000; Leo and Hansch, 1971). Based on these findings, LID was used as a model penetrant in the present study.

LID contains an amino group (p*Ka* 7.8, JPEC, 2010), and the fraction of ionization is known to vary depending on the pH of the formulation. In the present study, the unionized fractions accounted for 0.16, 28.5 and 99.4% in the pH 5.0, 7.4, and 10 donor solutions respectively. The cumulative amount of LID that permeated through full-thickness skin increased with an increase in the fraction of the unionized form of LID in the donor solution (Fig. 2). When the compound exists as unionized and ionized compound forms, the total permeability coefficient (P) can be described as follows (Hayashi et al., 1992)

$$P = \frac{C_u P_u + C_i P_i}{C_u + C_i} \tag{4}$$

where C_u and C_i are the concentrations in the donor solution, and P_u and P_i are the

permeability coefficients for the unionized and ionized forms. The permeation rate of the unionized and ionized forms of LID from the pH 7.4 donor solution through full-thickness skin (C_uP_u and C_iP_i) was calculated using equation (4). The resulting values of C_uP_u and C_iP_i were 7.1×10^{-4} and 3.4×10^{-5} cm/s, which revealed the significantly lower skin permeability of the ionized form than of the unionized one. The SC, which is the main permeation barrier of full-thickness skin, is considered as a lipophilic membrane; therefore, permeation through the SC may be difficult for ionized LID (Swarbrick et al., 1992; Hatanaka et al., 1995; Hatanaka et al., 1996). The pH values of the VED before and after the permeation experiments were approximately 7.4, regardless of the applied donor solutions (Table 2), and both the unionized and ionized forms of LID permeated through these layers. On the other hand, the difference in LID permeated from donor solutions having various pH values was lower for stripped skin than for full-thickness skin (Fig. 2); therefore permeation of ionized LID cannot be ignored for stripped skin.

The LID concentration-depth profile for full-thickness skin (Fig. 5) was typical for the two-layered skin permeation model shown in Fig. 1. Because the concentration ratio of the Line segment **ab** against **bc** at the surface between the SC and VED represented the permeation resistance ratio of the SC against the VED, the ratio of the

concentration at $\boldsymbol{x} = \boldsymbol{L_{sc}}$ against that at $\boldsymbol{x} = \mathbf{0}$ in the SC should signify the permeability coefficient ratio of stripped skin against full-thickness skin (Sugibayashi et al., 2010). The concentration ratio of the surface against the dermis side of the SC was 0.061 (Fig. 3), while the permeability coefficient ratio was 0.056 (Fig. 2, Table 1). Based on the two-layered model, skin permeation parameters were determined from the corresponding permeation data through full-thickness and stripped skins, and LID concentrations at various skin depths were subsequently calculated using these parameters. LID concentrations as well as the mean skin concentration could be predicted at each depth (Figs. 3-5) (Sugibayashi et al., 2010).

Although skin permeation parameters were obtained from animal experiments in the present study, these parameters can be predicted using the physicochemical properties of compounds (Hatanaka et al., 1990; Potts and Guy, 1992; Geinoz et al., 2004). Skin concentration-depth profiles may also be predicted without animal experiments, such that animal species differences can be disregarded (Bartek et al., 1972; Bronaugh et al., 1982; Sato et al., 1989).

In the present study, LID, which is relatively lipophilic, was used as the model penetrant. Since the skin is a lipophilic two-layered membrane, the prediction of skin concentration-depth profiles may be insufficient for hydrophilic compounds. (Feldmann

and Maibach, 1967; Ogiso et al., 2002; Oshizaka et al., 2012). The contribution of appendages or the hydrophilic pathway (Hatanaka et al, 1990) must be considered for more accurate predictions. Furthermore, because predictions were only made under steady state permeation in this study, comprehensive dermatokinetics including non-steady state permeation are required.

In conclusion, penetrant concentration-skin depth profiles can be predicted easily by analyzing skin permeation data according to Fick's diffusion law. This method will be useful for promoting the efficient preparation of topically applied drugs and cosmetics.

References

Bartek, M.J., LaBudde, J.A., Maibach, H.I., 1972. Skin permeability in vivo: comparison in rat, rabbit, pig and man. J. Invest. Dermatol. 58, 114-123.

Bos, J.D., Meinardi, M.M., 2000. The 500 Dalton rule for the skin permeation of chemical compounds and drugs. Exp. Dermatol. 9, 165-169.

Bronaugh, R.L., Stewart, R.F., Congdon, E.R., 1982. Methods for in vitro percutaneous absorption studies II: animal models for human skin. Toxicol. Appl. Pharmacol. 62,

481-488.

Feldmann, R.J., Maibach, H.I., 1967. Regional variation in percutaneous penetration of 14C cortisol in man. J. Invest. Dermatol. 48, 181-183.

Geinoz, S., Guy, R.H., Testa, B., Carrupt, P.A., 2004. Quantitative structure-permeation relationships (QSPeRs) to predict skin permeation: a critical evaluation. Pharm. Res. 21, 83-92.

Hatanaka, T., Inuma, M., Sugibayashi, K., Morimoto, Y., 1990. Prediction of skin permeability of drugs. I. Comparison with artificial membrane. Chem. Pharm. Bull. 38, 3452-3459.

Hatanaka, T., Katayama, K., Koizumi, T., Sugibayashi, K., Morimoto, Y., 1994. In vitro-in vivo correlation of percutaneous absorption: isosorbide dinitrate and morphine hydrochloride. Biol. Pharm. Bull. 17, 826-830.

Hatanaka, T., Morigaki, S., Aiba, T., Katayama, K., Koizumi, T., 1995. Effect of pH on the skin permeability of a zwitterionic drug, cephalexin. Int. J. Pharm. 125, 195-203.

Hatanaka, T., Kamon, T., Uozumi, C. Morigaki, S., Aiba, T., Katayama, K., Koizumi, T., 1996. Influence of pH on skin permeation of Amino Acids. J. Pharm. Pharmacol. 48, 675-679.

Hayashi, T., Sugibayashi, K., Morimoto, Y., 1992. Calculation of skin permeability

coefficient for ionized and unionized species of indomethacin. Chem. Pharm. Bull. 40, 3090-3093.

Huffman, D.H., Crow, J.W., Pentikainen, P. Azarnoff, D.L., 1976. Association between clinical cardiac status, laboratory parameters, and digoxin usage. Am. Heart J. 91, 28-34.

JPEC (Japanease Pharmacists Education Center), 2010. JPDI (The Japanese Pharmacopoeia 16th ed. Drug Information). Jiho, Tokyo.

Kalia, Y.N., Pirot, F., Guy, R.H., 1996. Homogeneous transport in a heterogeneous membrane: water diffusion across human stratum corneum in vivo. Biophys. J. 71, 2692-2700.

Kano, S., Sugibayashi, K., 2006. Kinetic analysis on the skin disposition of cytotoxicity as an index of skin irritation produced by cetylpyridinium chloride: comparison of in vitro data using a three-dimensional cultured human skin model with in vivo results in hairless mice. Pharm. Res. 23, 329-335.

Kiistala, U., 1968. Suction blister device for separation of viable epidermis from dermis. J. Invest. Dermatol. 50, 129-137.

Klang, V., Schwarz, J.C., Lenobel, B., Nadj, M., Auböck, J., Wolzt, M., Valenta, C., 2012. In vitro vs. in vivo tape stripping: validation of the porcine ear model and

penetration assessment of novel sucrose stearate emulsions. Eur. J. Pharm. Biopharm. 80, 604-614.

Kligman, L.H., 1989. The ultraviolet-irradiated hairless mouse: a model for photoaging. J. Am. Acard. Dermatol. 21, 623-631.

Lademann, J., Meinke, M.C., Schanzer, S., Richter, H., Darvin, M.E., Haag, S.F., Fluhr, J.W., Weigmann, H.J., Sterry, W., Patzelt, A., 2012. In vivo methods for the analysis of the penetration of topically applied substances in and through the skin barrier. Int. J. Cosmet. Sci. 34, 551-9.

Leo, A., Hansch, C., 1971. Linear free-energy relationships between partitioning solvent systems. J. Org. Chem. 36, 1539-1544.

Maeda, K., Fukuda, M., 1996. Arbutin: mechanism of its depigmenting action in human melanocyte culture. J. Pharmacol. Exp. Ther. 276, 765-769.

Mishima, Y., Hatta, S., Ohyama, Y., Inazu, M., 1988. Induction of melanogenesis suppression: cellular pharmacology and mode of differential action. Pigment Cell Res. 1, 367-374.

Nakamura, A., Mori, D., Tojo, K. 2012. Evaluation of the predicted time-concentration profile of serum tulobuterol in human after transdermal application. Chem. Pharm. Bull. 60, 300-305.

N'Dri-Stempfer, B., Navidi, W.C., Guy, R.H., Bunge, A.L., 2009. Improved bioequivalence assessment of topical dermatological drug products using dermatopharmacokinetics. Pharm. Res. 26, 316-328.

Ogiso, T., Shiraki, T., Okajima, K., Tanino, T., Iwaki, M., Wada, T., 2002. Transfollicular drug delivery: penetration of drugs through human scalp skin and comparison of penetration between scalp and abdominal skins in vitro. J. Drug Target 10, 369-378.

Ohmori, S., Hayashi, T., Kawase, M., Saito, S., Sugibayashi, K., Morimoto, Y., 2000. Transdermal delivery of the potent analgesic dihydroetorphine: kinetic analysis of skin permeation and analgesic effect in the hairless rat. J. Pharm. Pharmacol. 52, 1437-1449.

Oshizaka, T., Todo, H., Sugibayashi, K., 2012. Effect of direction (epidermis-to-dermis and dermis-to-epidermis) on the permeation of several chemical compounds through full-thickness skin and stripped skin. Pharm. Res. 29, 2477-2488.

Pershing, L.K., Silver, B.S., Krueger, G.G., Shah, V.P., Skelley, J.P., 1992. Feasibility of measuring the bioavailability of topical betamethasone dipropionate in commercial formulations using drug content in skin and a skin blanching bioassay. Pharm. Res. 9, 45-51.

Potts, R.O., Guy, R.H., 1992. Predicting skin permeability. Pharm. Res. 9, 663-669.

Rougier, A., Dupuis, D., Lotte, C., Roguet, R., Schaefer, H., 1983. In vivo correlation between stratum corneum reservoir function and percutaneous absorption. J. Invest. Dermatol. 81, 275-278.

Sato, K., Oda, T., Sugibayashi, K., Morimoto, Y., 1988a. Estimation of blood concentration of drugs after topical application from in vitro skin permeation data I: prediction by convolution and confirmation by deconvolution. Chem. Pharm. Bull. 36, 2232-2238.

Sato, K., Oda, T., Sugibayashi, K., Morimoto, Y., 1988b. Estimation of blood concentration of drugs after topical application from in vitro skin permeation data II: approach by using diffusion model and compartment model. Chem. Pharm. Bull. 36, 2624-2632.

Sato, K., Sugibayashi, K., Morimoto, Y., Omiya, H., Enomoto, N., 1989. Prediction of the in-vitro human skin permeability of nicorandil from animal data. J. Pharm. Pharmacol. 41, 379-383.

Schaefer, H., Stüttgen, G., Zesch, A., Schalla, W., Gazith, J., 1978. Quantitative determination of percutaneous absorption of radiolabeled drugs in vitro and in vivo by human skin. Curr. Probl. Dermatol. 7, 80-94.

Seiji, M., Fitzpatrick, T.B., Birbeck, M.S., 1961. The melanosome: a distinctive subcellular particle of mammalian melanocytes and the site of melanogenesis. J. Invest. Dermatol. 36, 243-252.

Sheiner, L.B., Rosenberg, B., Marathe, W., 1977. Estimation of population characteristics of pharmacokinetic parameters from routine clinical data. J. Pharmacokin. Biopharm. 5, 445-479.

Sugibayashi, K., Todo, H., Oshizaka, T., Owada, Y., 2010. Mathematical model to predict skin concentration of drugs: toward utilization of silicone membrane to predict skin concentration of drugs as an animal testing alternative. Pharm. Res. 27, 134-142.

Surber, C., Wilhelm, K.P., Hori, M., Maibach, H.I., Guy, R.H., 1990. Optimization of topical therapy: partitioning of drugs into stratum corneum. Pharm. Res. 7, 1320-1324.

Surber, C., Wilhelm, K.P., Bermann, D., Maibach, H.I., 1993. In vivo skin penetration of acitretin in volunteers using three sampling techniques. Pharm. Res. 10, 1291-1294.

Swarbrick, J., Lee, G., Brom, J., Gensmantel, N.P. 1984. Drug permeation through human skin II: Permeability of ionizable compounds. J. Pharm. Sci. 73, 1352-1355.

Tojo, K., Lee, A.C., 1989. A method for predicting steady-state rate of skin penetration in vivo. J. Invest. Dermatol. 92, 105-108.

Vozeh, S.R., Hillman, R., Wandell, M., Ludden, T., Sheiner, L., 1985. Computer-assisted drug assay interpretation based on Bayesian estimation of individual pharmacokinetics: application to lidocaine. Ther. Drug Monit. 7, 66-75.

1

Table 1

Skin permeation parameters of LID

	P_{tot} (cm/s)	P_{ved} (cm/s)	K_{sc}	K_{ved}
pH 5.0	4.7×10^{-8}	1.5×10^{-5}	0.098	2.6
pH 7.4	2.4×10^{-6}	4.3×10^{-5}	7.2	7.3
pH 10	2.5×10^{-6}	6.0×10^{-5}	7.9	7.5

2

3

1

Table 2

pH values on the surface and dermis sides of skin before and after the permeation experiments[a]

	Full-thickness skin				Stripped skin		
	Before	After			After		
		pH 5.0	pH 7.4	pH 10	pH 5.0	pH 7.4	pH 10
Stratum corneum	6.2 ± 0.033	6.0 ± 0.058	6.2 ± 0.088	8.8 ± 0.058	-	-	-
Viable epidermis	7.4 ± 0.033	7.4 ± 0.088	7.4 ± 0.0	7.4 ± 0.058	7.1 ± 0.15	7.3 ± 0.058	9.8 ± 0.033
Dermis	7.5 ± 0.12	7.3 ± 0.033	7.3 ± 0.033	7.9 ± 0.033	7.4 ± 0.033	7.3 ± 0.033	8.9 ± 0.058

2 [a]Each value represents the mean ± S.E. of 3 experiments.

3

Fig. 1. Schematic diagram of the concentration-depth profile in the two-layered diffusion model. C_v is the penetrant concentration in vehicle, K_{sc} is the partition coefficient of the penetrant from vehicle to the SC, L_{sc} and L_{ved} are the thicknesses of the SC and VED, respectively.

Fig. 2. Cumulative amounts of LID that permeated through full-thickness (a) and stripped skins (b) from donor solutions at several pHs. Each value represents the mean ± S.E. of 3 experiments.

Fig. 3. Steady state LID concentrations at various depths in the SC (a) and those normalized by the SC thickness (b) after the application of pH 7.4 donor solution. Each symbol represents individual skin. The dashed line is the concentration calculated by equation (2) using permeation parameters.

Fig. 4. Steady state LID concentrations at various depths in the VED (a) and those normalized by the VED thickness (b) after the application of pH 7.4 donor solution. Each symbol represents individual skin. The dashed line is the concentration calculated by equation (3) using permeation parameters.

Fig. 5. Steady state LID concentration-depth profile for full-thickness skin after the application of pH 7.4 donor solution. This profile was constructed by combining data from Fig. 3d and Fig. 4f.

Fig. 1

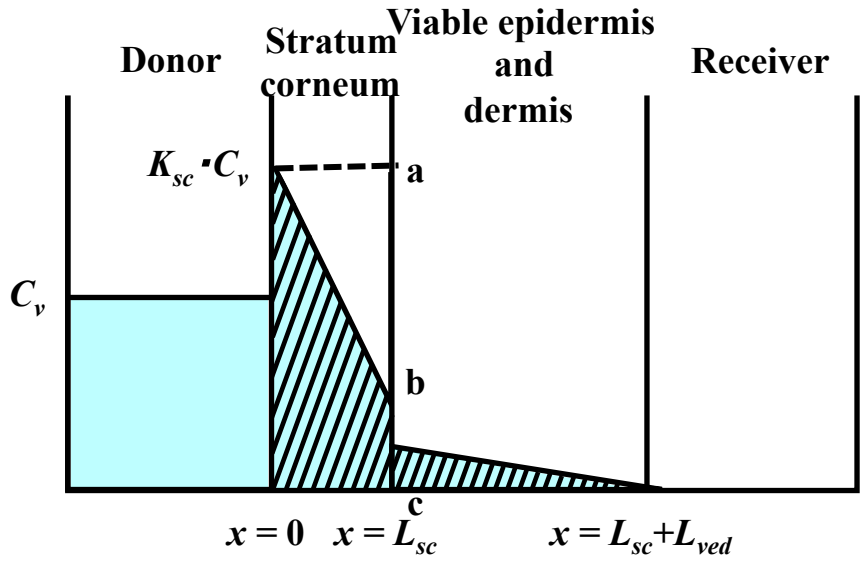
Donor
Stratum corneum
Viable epidermis and dermis
Receiver
$K_{sc} \cdot C_v$
a
C_v
b
c
$x = 0$
$x = L_{sc}$
$x = L_{sc}+L_{ved}$

Fig. 2

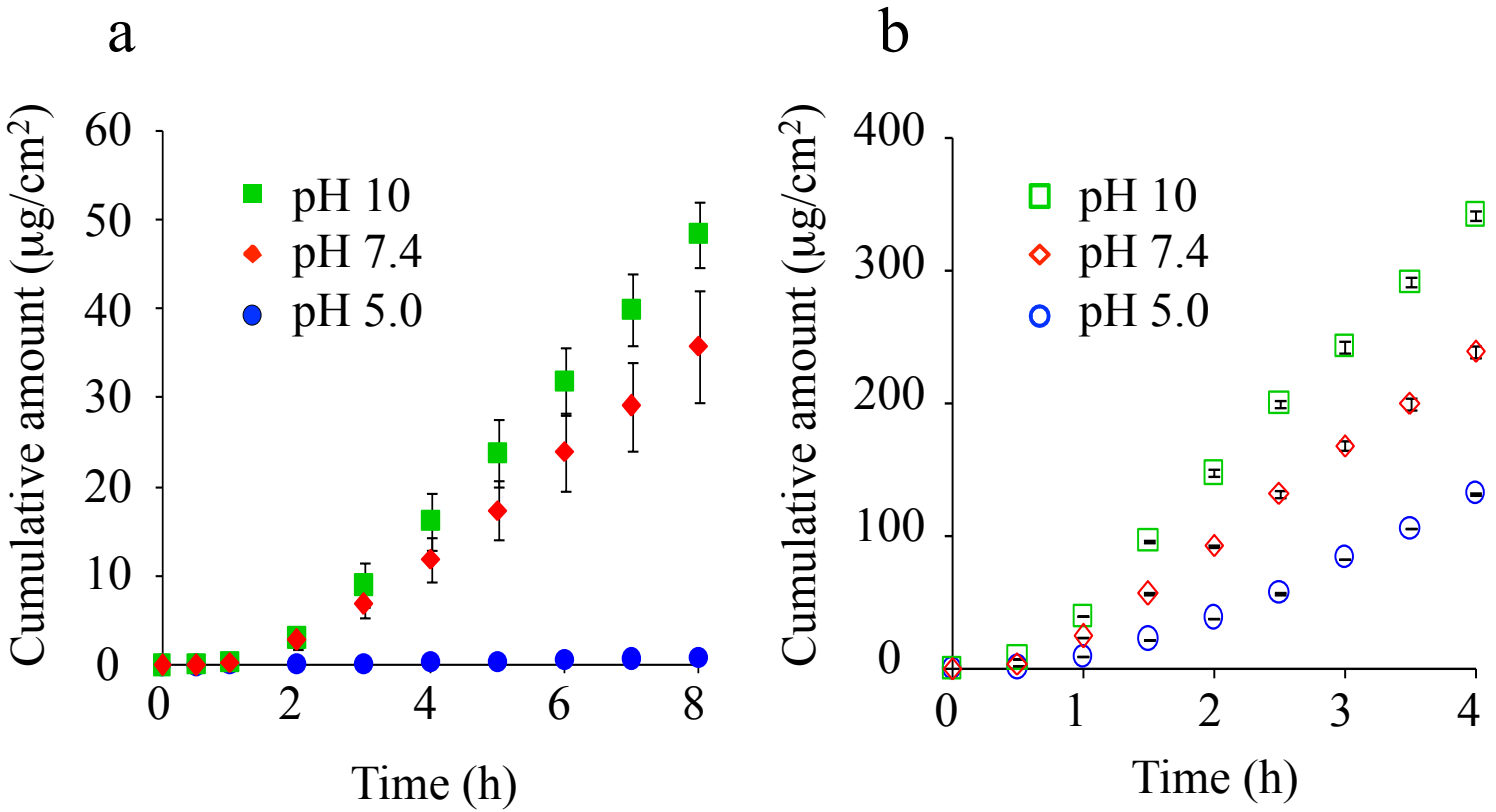
a
b
Cumulative amount (μg/cm²)
pH 10
pH 7.4
pH 5.0
Time (h)
0
10
20
30
40
50
60
100
200
300
400
2
4
6
8
1
3

Fig. 3

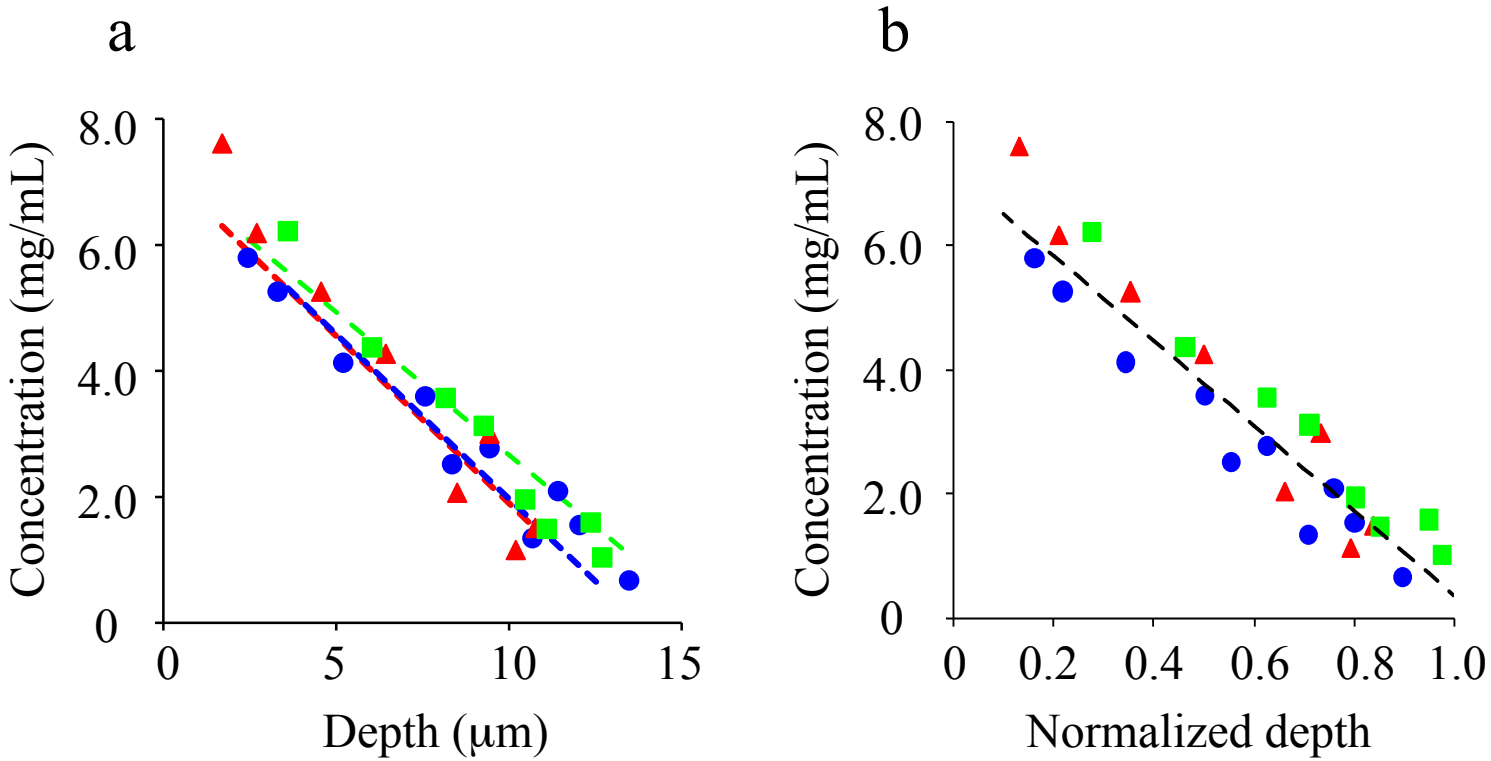
a
b
Concentration (mg/mL)
8.0
6.0
4.0
2.0
0
0
5
10
15
Depth (μm)
Concentration (mg/mL)
8.0
6.0
4.0
2.0
0
0
0.2
0.4
0.6
0.8
1.0
Normalized depth

Fig. 4

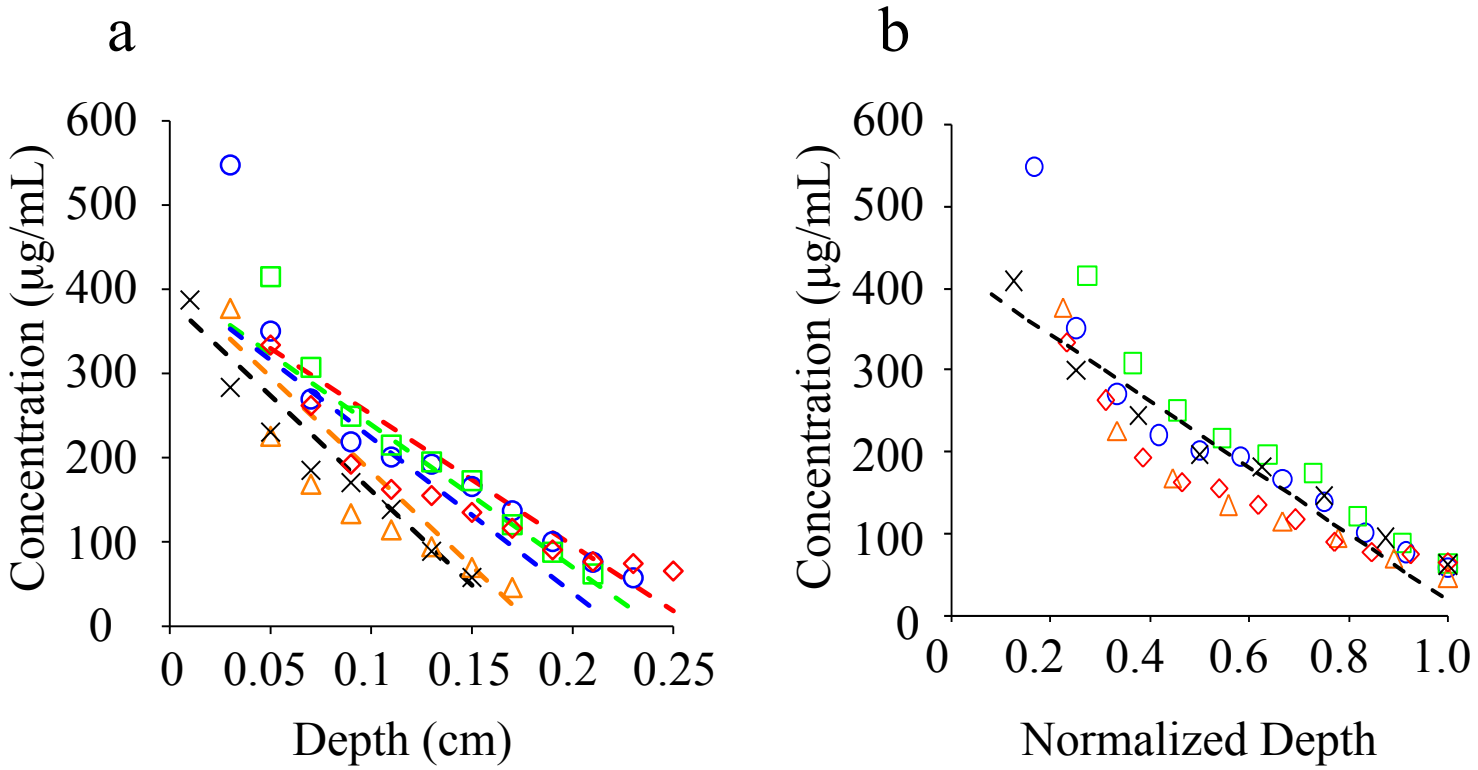
a
b
Concentration (µg/mL)
600
500
400
300
200
100
0
0
0.05
0.1
0.15
0.2
0.25
Depth (cm)
0.2
0.4
0.6
0.8
1.0
Normalized Depth

Fig. 5

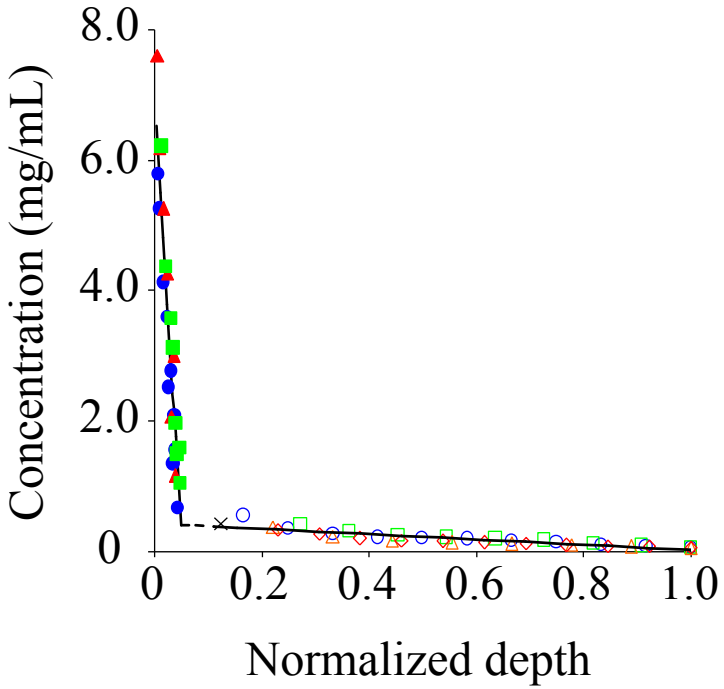
8.0
6.0
4.0
2.0
0
Concentration (mg/mL)
0
0.2
0.4
0.6
0.8
1.0
Normalized depth